CATTANEO-CHRISTOV HEAT FLUX EFFECT ON SAKIADIS MAGNETOHYDRODYNAMIC BOUNDARY-LAYER TRANSPORT PHENOMENA IN THE JEFFREY FLUID

by

Zarith Sofiah OTHMAN [a,c], ***Zailan SIRI*** [a,b], ***Muhamad Hifzhudin Noor AZIZ*** [a,b], ***and Kohilavani NAGANTHRAN*** [a,b*]

[a] Institute of Mathematical Sciences, Faculty of Science, Universiti Malaya, Kuala Lumpur, Malaysia
[b] Center for Data Analytics Consultancy & Services, Faculty of Science, Universiti Malaya, Kuala Lumpur, Malaysia
[c] Centre of Foundation Studies, Universiti Teknologi MARA, Cawangan Selangor, Kampus Dengkil, Dengkil, Selangor, Malaysia

Original scientific paper
https://doi.org/10.2298/TSCI221013214O

This study aims to perform a numerical simulation of the boundary flow with the characteristic Sakiadis flow of the MHD Jeffrey fluid under the Cattaneo-Christov heat flux model over the horizontal plate. The similarity transformation for the local similarity solution was used to reduce the set of governing equations to non-linear ODE. The equations were solved by using 'dsolve' command with the numeric option for the boundary value problem in MAPLE. Simulations have been carried out for different values of the relaxation retardation times, the Deborah number, the magnetic field parameter, the heat flux relaxation time, the Prandtl number, and the Schmidt parameter. A comparative study of the numerical results from the previously published paper with the present result for the dimensionless velocity gradient over the horizontal plate shows excellent agreement. It has been found that the growth of the Deborah number leads to the dimensionless velocity gradient enhancement, while the increment of the relaxation retardation times parameter and the magnetic field parameter indicates the opposite trend. The heat transfer rate noticeably decreased with an increment in the Prandtl number and thermal relaxation time at the fluid regime. Also, fluid concentration decreases with larger values of the Schmidt parameter.

Key words*: Cattaneo-Christov heat flux model, Jeffrey fluid, Sakiadis flow, MHD*

Introduction

Ensuring an optimal cooling rate during the manufacturing process is crucial for maintaining the desired quality of the final product. To achieve this, a controlled cooling system is necessary. An electrically polymeric liquid seems to be a good candidate for such applications of polymer and metallurgy because here, the flow can be controlled by an applied magnetic field [1]. The MHD flows play a significant role in various fields, including MHD power generation systems, nuclear reactor cooling, plasma studies, and geothermal energy extraction. The MHD effect arises when a magnetic field influences fluid-flow. Hartmann and Lazarus [2] were

* Corresponding author, e-mail: kohi@um.edu.my

the first people to arise come up with the idea of a combination between electromagnetic and hydrodynamic. Alfven [3] expanded the work done by Hartmann and Lazarus [2] by considering the conducting fluid under a constant magnetic field and proving that every fluid movement produces electric currents. He suggested that the existence of these waves may be important in the field of solar physics. Sarpkaya [4] expanded the work done by Alfven [3] and found that the fluid velocity distribution is more uniform when the fluid is placed in a magnetic field between two parallel planes. Sarpkaya [4] also investigated two fluid models: the power-law and Bingham plastic models. The word MHD is a combination of three words: magneto means magnetic field, hydro means water, and dynamic means movement or flow. The terms MHD and hydromagnetic are interchangeable and have the same meaning. Heat transfer analysis for MHD viscous fluid past a non-linear shrinking sheet was done by Javed *et al.* [5]. They found that for increasing magnetic field parameters, the fluid velocity for the first solution increases but decreases for the second solution by employing the Keller-Box method. Alamri *et al.* [6] studied the MHD second-grade fluid and Cattaneo-Christov heat flux models over a stretching cylinder. It is shown that the fluid velocity decreases when increasing the magnetic field parameter from 0 to 1. Recently, Asmadi *et al.* [7] found that increasing the Hartman number decreases the velocity profile.

The Jeffrey fluid model, as a subfamily of non-Newtonian fluids, has garnered significant attention in addressing the present problem. This fluid model represents a viscoelastic non-Newtonian fluid with both relaxation and retardation effects, making it an interesting subject of study. Researchers have extensively explored the impact of magnetic fields on this specific fluid-flow type. In recent studies, several researchers have focused on investigating various aspects of MHD flows and their associated heat transfer characteristics. For instance, Zokri *et al.* [8] conducted a study on the MHD Jeffrey fluid influence of radiation and viscous dissipation over a stretching sheet with convective boundary conditions. The findings of their study revealed that the magnetic parameter had a notable effect on the skin friction coefficient and the local Nusselt number. Specifically, the results demonstrated that an increase in the magnetic parameter led to a decrease in both the skin friction coefficient and the local Nusselt number. Mohd *et al.* [9] conducted a study on MHD mixed convection, specifically investigating the combination of a Jeffrey fluid (non-Newtonian fluid) with the Buongiorno model (nanofluid) over an inclined stretching sheet. They employed the Runge-Kutta-Fehlberg (RKF45) numerical method to generate accurate numerical results. Their research sheds light on the intricacies of heat and fluid-flow in such systems. In a related study, Hayat *et al.* [10] focused on the MHD Jeffrey nanofluid-flow with heat transfer over a stretching surface. The findings of this study indicated that an increase in the magnetic parameter resulted in a decrease in fluid velocity. These investigations contribute to our understanding of the complex behaviour of MHD flows and provide valuable insights into the influence of magnetic fields on the flow characteristics of Jeffrey fluids Additionally, Ullah *et al.* [11] delved into the thermal diffusion aspects of a 2-D and unsteady Jeffrey nanofluid, considering time-dependent thermal conductivity. They utilised the homotopy analysis method to compute dimensionless equations, revealing the enhanced utilisation of variable thermal conductivity due to the heat transportation of nanoparticles.

Numerical approaches play a crucial role in solving MHD equations by discretizing them and employing computational methods. Various numerical methods have been utilised for MHD problems, including finite volume methods [12], finite element methods [13, 14], and finite difference methods [15]. These methods enable the simulation and visualisation of fluid dynamics, magnetic field development, and energy transfer in MHD systems. They are particularly effective in addressing complex non-linear problems that lack analytical solutions. In addition the men-

tioned studies, there have been several recent investigations exploring different aspects of fluid dynamics and mathematical techniques. For instance, Hussain *et al.* [16] applied the shooting approach to analyse the peristaltic flow of a Jeffrey fluid in a curved channel. Utilizing the wavelength approximation, they obtained solutions for velocity and pressure distributions, examining the impact of various parameters such as curvature and Jeffrey fluid properties on flow characteristics. This study offered valuable insights into the peristaltic behaviour of Jeffrey fluids in curved channels. Another study by Ullah *et al.* [17] focused on the unsteady 2-D squeezing flow of MHD Jeffrey fluid between parallel plates. The researchers considered the influence of the Cattaneo-Christov heat flux model and employed the Levnberg-Marquardt method and ANN to solve the resulting system of equations. Through their analysis, they observed that an increase in the applied magnetic field strength led to a reduction in the velocity profile. Next, Ibrahim and Abou-Zeid [18] investigated the fluid temperature and concentration in MHD peristaltic transport of Jeffrey fluid using a computational simulation method called the adaptive shooting method. This technique, which utilises the direct adaptive shooting technique, allows for the accurate approximation of solutions to boundary value problems (BVP) involving highly non-linear systems of differential equations. The AST approach has proven to be effective in handling complex mathematical problems where analytical solutions are challenging to obtain. Moreover, MATLAB offers a user-friendly and accessible function called bvp4c, which is proficient in tackling complex problem-solving tasks. The bvp4c function is a computational tool that utilizes an iterative method for solving non-linear systems of equations. Its implementation is based on the Lobatto IIIa formula, a three-stage numerical integration technique widely recognized for its accuracy and efficiency. Naganthran *et al.* [19] examined the transport phenomena of the Jeffery fluid near the stagnation region over a radially stretching or shrinking disc. Through the utilization of the powerful and intuitive bvp4c function in MATLAB, dual solutions have been identified. In the present work, the MAPLE 21 application has been chosen to find the numerical results because of its simplicity and effectiveness in obtaining accurate numerical results. It offers an easy-to-use command in MAPLE 21 to find the desired results directly. Another study by Murali and Babu [20] investigated the numerical study of convective MHD Jeffrey fluid-flow between vertical plates with variable suction. The findings indicated that an increase in the magnetic field parameter led to the suppression of the fluid's primary velocity profiles. Furthermore, Omohkuale and Dange [15] explored the impact of heat absorption on unsteady MHD convective Jeffrey fluid-flow over an infinite vertical plate. The study revealed that the momentum boundary-layer increased with higher values of heat absorption and Jeffery parameters, while the fluid velocity decreased with higher values of suction and chemical reaction parameters.

The idea of examining heat transfer characteristics has revolved around the well-known Fourier Law of heat conduction for quite some time, proposed by Fourier [21]. This simplistic law may be used for a simple system but is unsuitable for a more complex set-up. The downside of this law is that a slight disturbance affects the fluid instantly due to the parabolic type of energy equation that the law produces. Subsequently, Maxwell, and Cattaneo made advancements to the model by introducing a relaxation time for heat flux. Furthermore, Christov [22] made additional refinements to the Maxwell-Cattaneo law by replacing the time derivative model with the Oldroyd upper convected derivative. This modification resulted in the development of material-invariant properties referred to as the Cattaneo-Christov heat flux. Cattaneo-Christov, a heat flux model, was previously used in many studies to investigate the coupled flow in a viscoelastic fluid [23], the Jeffrey fluid with homogeneous-heterogeneous reactions [24], the flow of Maxwell fluid in the presence of suction [25], and the third-order slip flow of viscoelastic nanofluid [26]. In the study conducted by Islam *et al.* [27], the MHD Maxwell

fluid-flow was measured using the Cattaneo-Christov heat flux model. They found that a higher unsteadiness parameter resulted in a reduction in the velocity profile while increasing the thermal and concentration profiles. The study also demonstrated that an increase in the magnetic parameters decreased the velocity profile of Maxwell fluid-flows. Tassaddiq [28] investigated the impact of hybrid nanoparticles on the thermal efficiency of nanostructured nanoparticles (micropolar fluid) using the Cattaneo-Christov heat flux model. This study sheds light on the influence of nanoparticle characteristics on the thermal behaviour of MHD fluids, expanding our understanding of heat transfer phenomena in such systems. Furthermore, in the study by Makinde *et al.* [29], it was observed that the thermal boundary-layer has a significant influence on the flow over a wedge compared to other geometries, such as a plate or a cone. Furthermore, Ramandevi *et al.* [30] indicates that the thermal relaxation time exhibits dual behaviour on the temperature of Casson fluid, and an increase in the temperature ratio or frictional heat leads to an increase in the thickness of the thermal boundary-layer. Thermal relaxation time is a characteristic of the fluid that determines how it responds to thermal changes, as it tends to restore thermal equilibrium and decrease the temperature of the fluid.

Despite the considerable advancements made by the Cattaneo-Christov theory, the current state of the literature indicates a lack of investigations regarding the influence of the Cattaneo-Christov heat flux model on MHD heat and mass transfer of Jeffrey fluid under Sakiadis flow conditions. Therefore, the objective of this article is to address this research gap. To achieve this, we employ a similarity transformation approach based on previously published work [31], and the resulting system of ODE is numerically solved using the BVP command in MAPLE Software. The outcomes of this study hold considerable importance for scientists and engineers, as they provide valuable insights into the analysis of convective heat and the integration of the Cattaneo-Christov heat flux model for mass transfer in the Sakiadis MHD boundary-layer flow of Jeffrey fluid. These findings enhance our understanding of the fundamental principles governing the phenomenon and enable accurate predictions of the convective flow properties of Jeffrey fluid in various advanced technical systems as well as industrial and engineering applications. Examples of such applications include hydrodynamics, metal extrusion, metal spinning, and manufacturing processes involving glass fibres.

Mathematical formulation

Flow analysis

A steady 2-D incompressible laminar flow of non-Newtonian fluid over a horizontal sheet and the chemical reaction, thermal radiation, and heat source effects subject to Sakiadis boundary-layer flow are considered. The constitutive equation for Jeffrey fluid is defined:

$$\tau = -pI + S \tag{1}$$

with τ is the Cauchy stress tensor, I – the identity tensor, p – the pressure, and S – the define as the extra stress tensor and it is written:

$$S = \frac{\mu}{1+\lambda_1}\left[R_1 + \lambda_2\left(\frac{\partial R_1}{\partial t} + \mathbf{V}\nabla\right)R_1\right] \tag{2}$$

where μ is the dynamic viscosity, λ_1 – the relaxation retardation time ratio, λ_2 – the retardation time, $\mathbf{V} = (u, v)$ – the Maxwell fluid's velocity vector, u and v are velocity components along the x- and y-directions, respectively, and R_1 – the Rivlin-Ericksen tensor defined:

$$R_1 = (\nabla\mathbf{V}) + (\nabla\mathbf{V})' \tag{3}$$

This model comprises the features of viscous fluid and second-grade fluid, which are: first, if $\lambda_1 = \lambda_2 = 0$ then the problem can be characterised as the viscous fluid model, next, if $\lambda_1 \neq 0$ and $\lambda_2 = 0$, then the problem can be represented as the second-grade fluid, and lastly, if $\lambda_1 \neq \lambda_2 \neq 0$, then the problem is known as the Jeffrey fluid model [32]. With several calculations and simplifications, the momentum equation of Jeffrey fluid in 2-D flow can be written:

$$\frac{\partial u}{\partial x} + \frac{\partial v}{\partial y} = 0 \tag{4}$$

$$u\frac{\partial u}{\partial x} + v\frac{\partial u}{\partial y} = \frac{\nu}{1+\lambda_1}\left(\frac{\partial^2 u}{\partial y^2} + \lambda_2\left[u\frac{\partial^3 u}{\partial x \partial y^2} + v\frac{\partial^3 u}{\partial y^3} - \frac{\partial u}{\partial x}\frac{\partial^2 u}{\partial y^2} + \frac{\partial u}{\partial y}\frac{\partial^2 u}{\partial x \partial y}\right]\right) - \frac{\sigma {B_0}^2}{\rho}u \tag{5}$$

where $\nu = \mu/\rho$ is the kinematic viscosity of the fluid, and ρ – the fluid density, B_0 – the uniform magnetic field, and σ – the electrical conductivity subject to the boundary conditions of Sakiadis flow:

$$u = U_\infty,\ v = 0 \text{ at } y = 0 \text{ and } u \to 0 \text{ as } y \to \infty \tag{6}$$

To simplify the flow model as presented previously, we introduce the similarity transformation:

$$\psi = \sqrt{U_\infty \nu x}\, f(\eta),\ \eta = \sqrt{\frac{U_\infty}{\nu x}}\, y \tag{7}$$

where f is the dimensionless stream function and ψ – the stream function defined as $u = \partial\psi/\partial y$ and $v = -(\partial\psi/\partial x)$. Then, let $U_\infty = cx$ where U_∞ is the linear velocity is, and c – the positive constant. Hence, eq. (7) is simplified to:

$$\psi = x\sqrt{c\nu}\, f(\eta),\ \eta = \sqrt{\frac{c}{\nu}}\, y \tag{8}$$

The single-stream function can be replaced by the velocity components u and v. It is chosen so that the continuity equation in eq. (4) is satisfied automatically:

$$u = cx\frac{\partial f}{\partial \eta},\ v = -\sqrt{c\nu}\, f(\eta) \tag{9}$$

Invoking eqs. (8) and (9) into eq. (5), the ordinary differential equation is obtained:

$$f''' + (1+\lambda_1)\left(ff'' - f'^2 - \mathrm{M}f'\right) + \beta\left(f''^2 - ff'''\right) = 0 \tag{10}$$

where $\beta = c\lambda_2$ is the Deborah number, which is also defined as a dimensionless number, often used in rheology to characterise the fluidity of materials under specific flow conditions, and lastly, $\mathrm{M} = \sigma B_0^2/c\rho$ is the magnetic field parameter, or the Hartmann number. The boundary conditions for eq. (6) are given:

$$f = 0,\ f' = 1 \text{ at } \eta = 0 \text{ and } f' = 0 \text{ at } \eta \to \infty \tag{11}$$

Heat transfer

The Maxwell-Cattaneo law introduced the relaxation time of the heat flux, λ_3 so that the effect of the governing equation could be changed to a form of the wave equation. The thermal flux vector becomes:

$$\left(1 + \lambda_3\frac{\partial}{\partial t}\right)\mathbf{q} = -k\nabla\mathbf{T} \tag{12}$$

where **q** is the heat flux and **T** – the temperature of the Maxwell fluid. To generalise Fourier law based on eq. (12), Christov [22] used Oldroyd's upper convected derivative to replace the partial time derivative. Hence, the material-invariant form for the internal energy is obtained:

$$\rho c_p\left(\frac{\partial T}{\partial t}+\mathbf{V}\nabla\boldsymbol{T}\right)=-\nabla\mathbf{q} \tag{13}$$

where c_p is the constant specific heat. Next, the frame-indifferent generalisation of Fourier's law with the addition of relaxation of the heat flux is defined:

$$\mathbf{q}+\lambda_3\left[\frac{\partial q}{\partial t}+\mathbf{V}\nabla\mathbf{q}-\mathbf{q}\nabla\mathbf{V}+\left(\nabla\mathbf{V}\right)\mathbf{q}\right]=-k\nabla\mathbf{T} \tag{14}$$

where k is the thermal conductivity. When $\lambda_3 = 0$, eq. (14) will be simplified to Fourier's law of heat conduction. Since the fluid in the present problem is incompressible, therefore, $\nabla\mathbf{V} = 0$. Tibullo and Zampoli [33], eq. (14) can then be written:

$$\mathbf{q}+\lambda_3\left[\frac{\partial q}{\partial t}+\mathbf{V}\nabla\mathbf{q}-\mathbf{q}\nabla\mathbf{V}\right]=-k\nabla\mathbf{T} \tag{15}$$

On the other hand, using the energy equation for the steady boundary-layer flow by Han *et al.* [23] and Khan *et al.* [34], we have:

$$\rho c_p\mathbf{V}\cdot\nabla\mathbf{T}=-\nabla\boldsymbol{q} \tag{16}$$

Finally, utilising eq. (15) in eq. (16), the temperature-governing equation is formulated:

$$u\frac{\partial T}{\partial x}+v\frac{\partial T}{\partial y}+\lambda_3\left[u^2\frac{\partial^2 T}{\partial x^2}+v^2\frac{\partial^2 T}{\partial y^2}+2uv\frac{\partial^2 T}{\partial x\partial y}+\left(u\frac{\partial u}{\partial x}+v\frac{\partial u}{\partial y}\right)\frac{\partial T}{\partial x}+\left(u\frac{\partial v}{\partial x}+v\frac{\partial v}{\partial y}\right)\frac{\partial T}{\partial y}\right]=\alpha\frac{\partial^2 T}{\partial y^2} \tag{17}$$

where α is the thermal diffusivity, and subject to the boundary conditions given:

$$T=T_w \text{ at } y=0 \text{ and } T\to T_\infty \text{ as } y\to\infty \tag{18}$$

where T_w is the temperature of the stretching sheet and T_∞ – the ambient temperature. Next, to derive eq. (17), we introduce the similarity transformation, the dimensionless temperature, θ of the form:

$$\theta\left(\eta\right)=\frac{T-T_\infty}{T_w-T_\infty} \text{ and } T=\theta(\eta)(T_w-T_\infty)+T_\infty \tag{19}$$

Using the similarity transformation of eqs. (8)-(10) and eq. (14), eq. (12) is reduced:

$$\frac{1}{\mathrm{Pr}}\theta''+f\theta'-\gamma\left(f^2\theta''+ff'\theta'\right)=0 \tag{20}$$

where the Prandtl number is given as $\mathrm{Pr} = \nu/\alpha$ wherein the kinematic viscosity, ν, divided by thermal diffusivity, α. The definition of kinematic viscosity is a diffusivity for velocity or momentum, while the definition of thermal diffusivity is a diffusivity for temperature or heat. The non-dimensional thermal relaxation time is given as $\gamma = c\lambda_3$. The boundary conditions for eq. (20):

$$\theta=1 \text{ at } \eta=0 \text{ and } \theta=0 \text{ at } \eta\to\infty \tag{21}$$

Mass transfer

Mass transfer arises from variations in the concentration of specific chemicals within a mixture. By using the principle of conservation of mass, the mass transfer that passes through the control element is the rate of mass-flow out of the control volume (outflow) subtracted from the rate of mass-flow into the control volume (inflow) plus the increase in mass, which is equal to zero. Through subsequent substitution and calculations, the concentration equation for the boundary-layer problem becomes:

$$u\frac{\partial C}{\partial x}+v\frac{\partial C}{\partial y}=D\frac{\partial^2 C}{\partial y^2} \tag{22}$$

subject to the boundary conditions:

$$C=C_w \text{ at } y=0 \text{ and } C\to C\infty \text{ as } y\to\infty \tag{23}$$

where C_w is the concentration of the stretching sheet and C_∞ is the ambient concentration. Next, by using similarity transformations and dimensionless concentration, ϕ of the form:

$$\phi(\eta)=\frac{C-C_\infty}{C_w-C_\infty} \text{ and } C=\phi(\eta)(C_w-C_\infty)+C_\infty \tag{24}$$

Equation (22) is reduced to:

$$\phi''+\mathrm{Sc}f\phi'=0 \tag{25}$$

where Sc = ν/D is the Schmidt parameter. The boundary conditions for eq. (25):

$$\phi=1 \text{ at } \eta=0 \text{ and } \phi=0 \text{ at } \eta\to\infty \tag{26}$$

The local skin friction coefficient, local Nusselt number, and local Sherwood number

The physical quantities of interest are the skin-friction coefficient, C_f, the local Nusselt number, Nu_x, and the local Sherwood number, Sh_x, which are defined:

$$C_f=\frac{\tau_w}{\rho U_\infty^2},\ \mathrm{Nu}_x=\frac{xq_w}{k\left(T_w-T_\infty\right)},\ \mathrm{Sh}_x=\frac{xq_m}{D\left(C_w-C_\infty\right)} \tag{27}$$

where τ_w, q_w, and q_m are the shear stress along the stretching surface, the surface heat flux, and the surface mass flux, respectively, which are given:

$$\tau_w=\mu\left(\frac{\partial u}{\partial y}\right)_{y=0},\ q_w=-k\left(\frac{\partial T}{\partial y}\right)_{y=0},\ q_m=-D\left(\frac{\partial C}{\partial y}\right)_{y=0} \tag{28}$$

with μ being the dynamic viscosity and k being the thermal conductivity. Dimensionless forms of skin friction coefficient, local Nusselt number, and local Sherwood number:

$$C_f\left(\mathrm{Re}_x\right)^{1/2}=f''(0),\ \mathrm{Nu}_x\left(\mathrm{Re}_x\right)^{-1/2}=-\theta'(0),\ \mathrm{Sh}_x\left(\mathrm{Re}_x\right)^{-1/2}=-\phi'(0) \tag{29}$$

where $\mathrm{Re}_x = U_\infty x/\nu$ is the local Reynolds number.

Results and discussion

The transformed governing eqs. (10), (20), and (25) along with the corresponding boundary eqs. (11), (21), and (26) are numerically solved using the dsolve/numeric/BVP command in MAPLE software [35]. To validate the accuracy of the proposed method, a comparison is made between the obtained results and those reported in previous studies, showing

favourable agreement. The skin friction coefficient is presented in tab. 1, including values from Andersson *et al*. [36], Chen [37], Babu and Narayana [38], and the current study for various magnetic parameters. It is observed that the skin friction coefficient decreases as the magnetic parameter increases. Based on tabs. 1-5, the relative percentage of errors is very close to 0%, and this indicates excellent agreement with the previous study.

Table 1. Comparison of the local skin friction coefficient for the various values of M with [36]

M	[36]	Present work	Relative error [%]
0.00	1.0000	1.00000	0.00000
0.50	1.2250	1.22474	0.02122
1.00	1.4140	1.41421	0.01485
1.50	1.5810	1.58114	0.00886
2.00	1.7320	1.73205	0.00289

Table 2. Comparison of the local skin friction coefficient for the various values of M with [37]

M	[37]	Present work	Relative error [%]
0.00	1.00000	1.00000	0.00000
0.50	1.22425	1.22474	0.04002
1.00	1.41421	1.41421	0.00000
1.50	1.58114	1.58114	0.00000
2.00	1.73205	1.73205	0.00000

The numerical computations are restricted entirely by the practical range of non-dimensional parameters, such as ($0.4 \leq \lambda_1 \leq 1.5$), ($0.2 \leq \beta \leq 0.6$), ($0.2 \leq \gamma \leq 0.6$), and ($0.1 \leq \mathrm{Sc} \leq 1.5$) [32] throughout all the results in this study. Meanwhile, the physical properties of the fluid are used to simulate the system in a real-life situation, in which parameters Prandtl numbers lie within ($1.5 \leq \mathrm{Pr} \leq 2.0$) as shown in tab. 6. Table 7 demonstrates the effect of changing some of the non-dimensional parameters in the model on the skin-friction factor coefficient, $f''(0)$, the local Nusselt number, $\theta'(0)$, and the local Sherwood number, $\phi'(0)$. The results show that $f''(0)$ increases while $-\theta'(0)$ and $-\phi'(0)$ decrease when both parameters λ_1 and M are increased. However, the results show the opposite trend when β is increased. The values of $-\phi'(0)$ are unchanged for different values of Prandtl number and γ since these two parameters are absent from the concentration equation, thus, varying these parameters does not affect the fluid's concentration profile. The values of $f''(0)$ and$-\theta'(0)$ remain fixed for different values of Shmidt number because the parameter only exists in the concentration equation, it does not affect the values of skin friction or the Nusselt number.

Table 3. Comparison of the local skin friction coefficient for the various values of M with[38]

M	[38]	Present work	Relative error [%]
0.00	1.00000	1.00000	0.00000
0.50	1.22479	1.22474	0.00408
1.00	1.41432	1.41421	0.00778
1.50	1.58115	1.58114	0.00063
2.00	1.73225	1.73205	0.01155

Table 4. Comparison values of $f''(0)$ when $M = Sc = \gamma = 0$ and $\lambda_1 = 0.2$

β	[39] (Exact)	Present work	Relative error [%]
0	−1.09544512	−1.09544576	0.00006
0.2	−1.00000000	−1.00000129	0.00013
0.4	−0.92582010	−0.92582232	0.00024
0.6	−0.86602540	−0.86602908	0.00042
0.8	−0.81649658	−0.81650173	0.00063
1.0	−0.77459667	−0.77460285	0.00080
1.2	−0.73854895	−0.73855880	0.00133
1.4	−0.70710678	−0.70711653	0.00138
1.6	−0.67936622	−0.67938034	0.00208

Table 5. Comparison values of $f''(0)$ when $M = Sc = \gamma = 0$ and $\beta = 0.2$

λ_1	[39] (Exact)	Present work	Relative error [%]
0.0	−0.91287093	−0.91287373	0.00031
0.4	−1.08012345	−1.08012390	0.00004
0.6	−1.15470054	−1.15470074	0.00002
0.8	−1.22474487	−1.22474497	$0.00008 \cdot 10^{-3}$
1.0	−1.29099445	−1.29099450	$0.00387 \cdot 10^{-3}$
1.2	−1.35400640	−1.35400661	0.00002
1.4	−1.41421356	−1.41421484	0.00009
1.6	−1.47196014	−1.47196502	0.00033

Table 6. The physical properties of the selected fluid

Fluid	Pr	T_∞	ν
Gaseous ammonia	1.5-2.0	298.15	0.145

Table 7. The variations of $f''(0)$, $-\theta'(0)$, and $-\phi'(0)$ for various values of non-dimensional governing parameters

β	λ_1	M	Pr	γ	Sc	$f''(0)$	$-\theta'(0)$	$-\phi'(0)$
0.2	0.5	0.5	1.5	0.6	1.5	−1.38902	−0.79241	−0.79869
0.4						−1.29083	−0.80091	−0.80621
0.6						−1.21266	−0.80842	−0.81224
0.3	0.5	0.5	1.5	0.6	1.5	−1.33671	−0.79649	−0.80261
	1					−1.53168	−0.77687	−0.78568
	1.5					−1.70633	−0.76138	−0.77155
0.3	0.5	0.5	1.5	0.6	1.5	−1.33671	−0.79649	−0.80261
		1				−1.52896	−0.77774	−0.78648
		1.5				−1.70314	−0.76242	−0.77255
0.3	0.5	0.5	1.5	0.6	1.5	−1.33671	−0.79649	−0.80261
			1.7			−1.33671	−0.84698	−0.80261
			2			−1.33671	−0.92648	−0.80260
0.3	0.5	0.5	1.5	0.2	1.5	−1.33671	−0.79897	−0.80261
				0.4		−1.33671	−0.79673	−0.80261
				0.6		−1.33671	−0.79649	−0.80261
0.3	0.5	0.5	1.5	0.6	0.5	−1.33670	−0.79649	−0.59685
					1	−1.33671	−0.79649	−0.69839
					1.5	−1.33671	−0.79649	−0.80261

Figures 1(a)-2(a) depict the effect of magnetic field parameters on the velocity profiles, $f'(\eta)$, temperature profiles, $\theta'(\eta)$, and concentration profiles, $\phi'(\eta)$. The velocity profile decays faster with an increase in the magnetic field parameter. From a physical point of view, when the magnetic field is applied to this fluid, the velocity of the Jeffrey fluid is distributed by the Lorenz force present in the fluid; this causes the fluid to move faster, and in turn, it tends to decelerate the fluid-flow. On the contrary, an increased magnetic field strength leads to a higher convergence rate of the thermal conductivity and concentration boundary-layers, as depicted in figs. 1(a) and 2(a). From this observation, it can be inferred that variations in the magnetic field parameters have a negligible impact on the velocity, temperature, and concentration profiles. Figure 2(b) expresses the effect of the Deborah number on the velocity profile $f'(\eta)$. Increasing the Deborah number causes the velocity profile to decay faster towards zero. On the other hand, the temperature profile and the concentration profile decrease with increasing parameters of β, as shown in figs. 3(a) and 3(b). The Deborah number is defined as the ratio of fluid relaxation time to its deformation rate. Hence, when the parameter β increases, the deformation time of the fluid decreases, and the relaxation time increases. As a result, it causes the thickness of momentum,

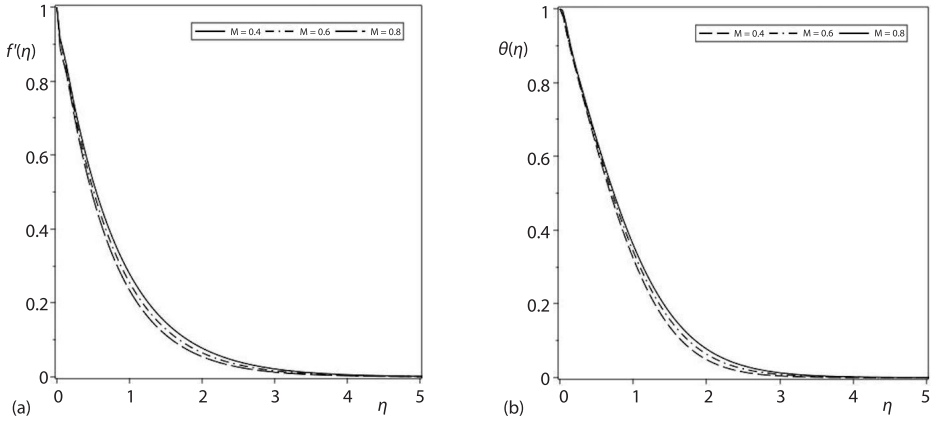

Figure 1. (a) Impact of M on $f'(\eta)$ and (b) impact of M on $\theta(\eta)$, when Pr = 1.5 = Sc, γ = 0.6, λ_1 = 0.5, and β = 0.3

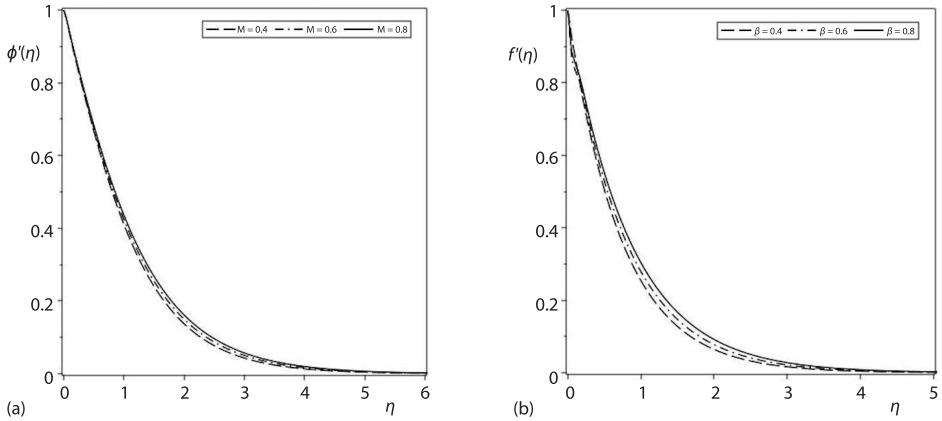

Figure 2. (a) Impact of M on $\phi(\eta)$ and (b) impact of β on $f'(\eta)$, when Pr = 1.5 = Sc, λ_1 = 0.5 = M, and γ = 0.6

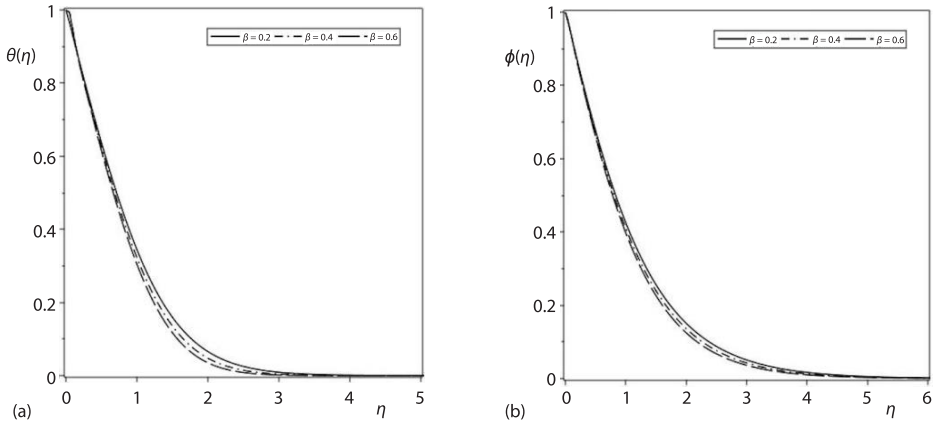

Figure 3. (a) Impact of β on $\theta(\eta)$ and (b) impact of β on $\phi(\eta)$, when Pr = 1.5 = Sc, λ_1 = 0.5 = M, and γ = 0.6

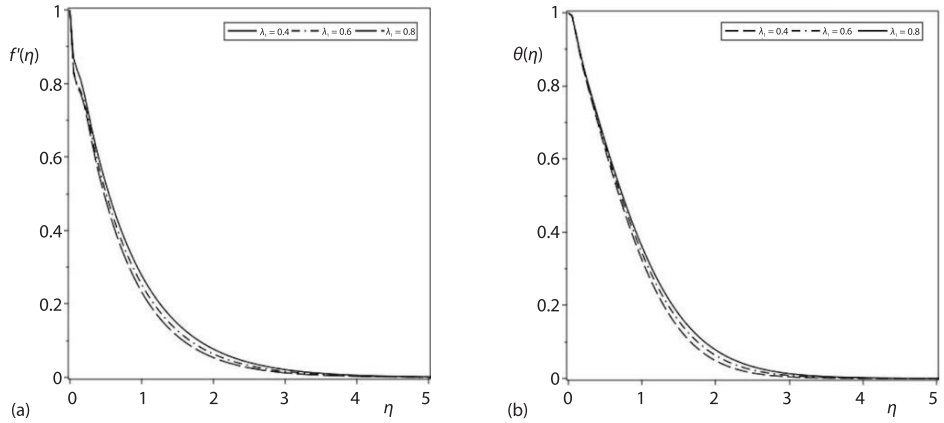

Figure 4. (a) Impact of λ_1 on $f'(\eta)$ and (b) impact of λ_1 on $\theta(\eta)$, when Pr = 1.5 = Sc, γ = 0.6, M = 0.5, and β = 0.3

the thermal boundary-layer, and the concentration boundary-layer to become thicker. It can be concluded that the changes in the parameter β affect the velocity, temperature, and concentration profiles slightly. Figure 4(a) illustrates the impact of parameter λ_1 on velocity profile $f'(\eta)$. The boundary-layer thickness declines with an increase in the ratio of relaxation retardation time of Jeffrey fluid. The outcomes of an increase in parameters λ_1 on the temperature profile $\theta'(\eta)$ and on the concentration profile $\phi'(\eta)$ are plotted in figs. 4(b) and 5(a), respectively. Both thermal and concentration boundary-layers are slightly increased with an increase in parameters λ_1.

Figure 5(b) clearly demonstrates the impact of a Prandtl number, increase on the temperature profile. As Prandtl numbers increases, the temperature gradient decreases. The Prandtl number is the ratio of momentum and thermal diffusivity. Hence, for higher Prandtl numbers, the momentum diffusivity terms lead to thermal diffusivity, and the fluid velocity is high enough to assist the heat transfer in the region and cause the heat dissipation occur quicker. Next, the impact of the increment in the non-dimensional thermal relaxation time γ is observed in fig. 6(a). There is a lower value of thermal conductivity in fluids when γ increases. Physically, it conveys that the time taken for the fluid to experience heat conduction gets longer, causing

the thermal boundary-layer to be thinner. In other words, heat dissipation occurs quickly. Figure 6(b) exhibits the effect of the Schmidt number, on the concentration profile. The Schmidt number is defined as the ratio of momentum diffusivity, which is analogous to the Prandtl number for the temperature gradient. As shown in fig. 6(b), when Schmidt number increases, momentum diffusivity dominates and the velocity of the fluid is high enough to facilitate mass distribution, which causes the concentration gradient to decrease faster.

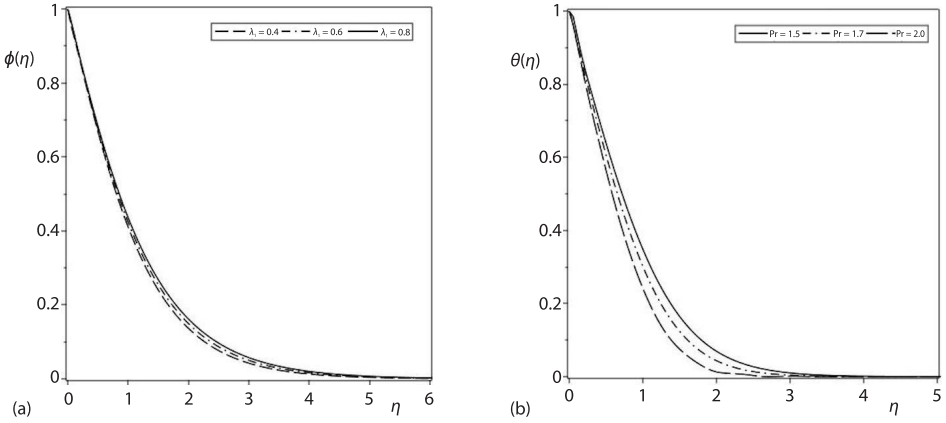

Figure 5. (a) Impact of λ_1 on $\phi(\eta)$ and (b) impact of Pr on $\theta(\eta)$, when Sc = 1.5, γ = 0.6, M = 0.5 = λ_1, and β = 0.3

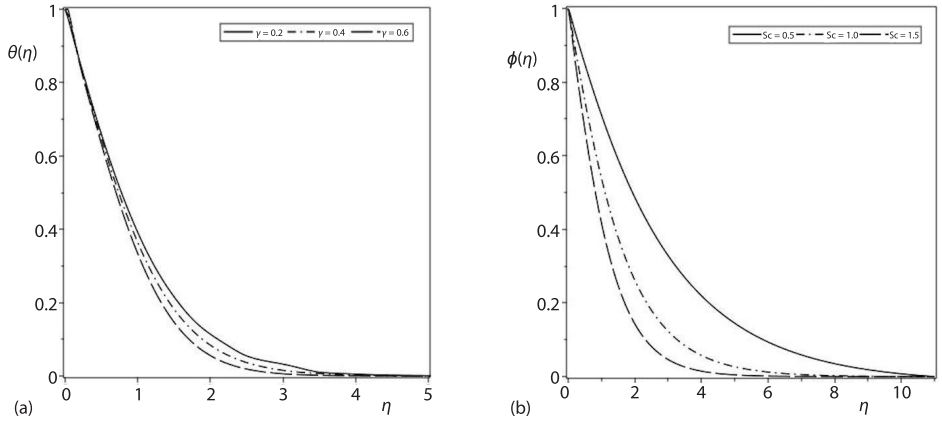

Figure 6. (a) Impact of γ on $\theta(\eta)$ and (b) impact of Sc on $\phi(\eta)$, when Pr = 1.5, γ = 0.5 = M = 0.5 = λ_1, and β = 0.3

Conclusions

The present study describes the boundary-layer flow of MHD Jeffrey fluid with the Cattaneo-Christov heat and mass transfer effect subject to the Sakiadis boundary flow. The main observations of this study are as follows.

- An increase in the Deborah number leads to a decrease in the thermal and concentration boundary-layer thickness.
- Increasing the Prandtl number reduces the temperature and thermal boundary-layer thickness.

- An increase in the non-dimensional thermal relaxation time results in a lower temperature.
- It is observed that concentration boundary-layer thickness decreases with increasing Schmidt numbers.

Acknowledgment

The authors would like to extend their deepest gratitude to the Malaysia Ministry of Education (Grant No. FRGS/1/2020/STG06/UM/02/4) for the financial and positive encouragement. K.N. would like to acknowledge UM's grant RMF1965-2021.

Nomenclature

B_0 – uniform magnetic field, [T]
c – positive constant, [–]
c_p – constant specific heat, [Jkg^{-1}K^{-1}]
C – mass concentration, [kgm^3]
C_w – concentration at the stretching sheet, [kgm^{-3}]
C_∞ – ambient concentration, [kgm^{-3}]
C_f – skin-friction coefficient, [–]
D – mass diffusion coefficient
f – dimensionless stream function, [–]
I – identity tensor, [–]
k – thermal conductivity, [Wm^{-1}K^{-1}]
M – magnetic field parameter or Hartmann number, [–]
Nu_x – local Nusselt number, [–]
Pr – Prandtl number, [–]
p – pressure, [Pa]
$\mathbf{q}$ – heat flux, [Wm^{-2}]
q_w – surface heat flux, [Wm^{-2}]
q_m – surface mass flux, [Wm^{-2}]
R_1 – Rivlin-Ericksen tensor, [Pa]
Re_x – local Reynolds number, [–]
S – extra stress tensor, [Pa]
Sc – Schmidt parameter, [–]
Sh_x – local Sherwood number, [–]
$\mathbf{T}$ – temperature of Maxwell fluid
T – fluid temperature, [K]
T_w – temperature of the stretching sheet, [K]
T_∞ – ambient temperature, [K]
U_∞ – linear velocity, [ms^{-1}]
u, v – velocity components along the x- and y-directions, respectively, [ms^{-1}]
$\mathbf{V}$ – velocity vector, [ms^{-1}]
x, y – Cartesian co-ordinates along the surface and normal to it, respectively, [m]

Greek symbols

α – thermal diffusivity, [Wm^{-1}K^{-1}]
β – Deborah number, [–]
γ – non-dimensional thermal relaxation time, [second]
θ – dimensionless temperature, [–]
λ_1 – relaxation retardation time ratio, [–]
λ_2 – retardation time, [second]
λ_3 – relaxation time of the heat flux, [second]
μ – dynamic viscosity, [kgm^{-1}s^{-1}]
ν – kinematic viscosity, [m^{2}s^{-2}]
ρ – fluid density, [kgm^{-3}]
σ – electrical conductivity, [Sm^{-1}]
τ – Cauchy stress tensor, [Pa]
τ_w – shear stress, [kgm^{-1}s^{-2}]
ψ – stream function, [–]

References

[1] Hayat, T., *et al*., Thermal and Concentration Stratifications Effects in Radiative Flow of Jeffrey Fluid over a Stretching Sheet, *PLoS ONE*., *9* (2014), 10, 107858
[2] Hartmann, J., Lazarus, F., Hg-Dynamics II: Theory of Laminar Flow of Electrically Conductive Liquids in a Homogeneous Magnetic Field, *Danske Videnskabernes Selskab*., *15* (1937), 7, pp. 1-45
[3] Alfven, H., Existence of Electromagnetic-Hydrodynamic Waves, *Nature*, *150* (1942), 3805, pp. 405-406
[4] Sarpkaya, T., Flow of Non-Newtonian Fluids in a Magnetic Field, *AIChE Journal*, *7* (1961), 2, pp. 324-328
[5] Javed, T., *et al*., Heat Transfer Analysis for a Hydromagnetic Viscous Fluid over a Non-Linear Shrinking Sheet, *Int. J. Heat Mass Transf*., *54* (2011), 9-10, pp. 2034-2042
[6] Alamri, S. Z., *et al*., Effects of Mass Transfer on MHD Second Grade Fluid Towards Stretching Cylinder: A Novel Perspective of Cattaneo-Christov Heat Flux Model, *Phys. Lett. A*., *383* (2019), 2-3, pp. 276-281
[7] Asmadi, M. S., *et al*., Convective Mass and Heat Transfer of Sakiadis Flow of Magnetohydrodynamic Casson Fluid over a Horizontal Surface Employing Cattaneo-Christov Heat Flux Model, *Malaysian J. Math. Sc*i., *15* (2021), 1, pp. 125-136
[8] Zokri, S. M., *et al*., Influence of Radiation and Viscous Dissipation on Magnetohydrodynamic Jeffrey Fluid over a Stretching Sheet with Convective Boundary Conditions, *Mal. J. Fund. Appl. Sci*., *13* (2017), 3, pp. 279-284

[9] Mohd, Z. S., *et al*., On Dissipative MHD Mixed Convection Boundary-Layer Flow of Jeffrey Fluid over an Inclined Stretching Sheet with Nanoparticles: Buongiorno Model, *Thermal Science*, *23* (2019), 6B, pp. 3817-3832
[10] Hayat, T., *et al*., Entropy Generation Optimization of MHD Jeffrey Nanofluid past a Stretchable Sheet with Activation Energy and Non-Linear Thermal Radiation, *Phys. A: Stat Mech Appl*., *544* (2020), 123437
[11] Ullah, K. S., *et a*l., Thermo Diffusion Aspects in Jeffrey Nanofluid over Periodically Moving Surface with Time Dependent Thermal Conductivity, *Thermal Science*, *25* (2021), 1A, pp. 197-207
[12] Vantieghem, S., *et al*., Applications of a Finite-Volume Algorithm for Incompressible MHD Problems, *Geophys J. Int*., *204* (2016), 2, pp. 1376-1395
[13] Dao, T. A., Nazarov, M., A High-Order Residual-Based Viscosity Finite Element Method for the Ideal MHD Equations, *Journal Sci. Comput*., *92* (2022), 3, 77
[14] Salmi, A., *et al*., Numerical Study of Heat and Mass Transfer Enhancement in Prandtl Fluid MHD Flow Using Cattaneo-Christov Heat Flux Theory, *Case Stud Therm Eng*., *33* (2022), 101949.
[15] Omokhuale, E., Dange, M. S., Heat Absorption Effect on Magnetohydrodynamic (MHD) Flow of Jeffery Fluid in an Infinite Vertical Plate, *Fudma J, Sci*., *7* (2023), 2, pp. 45-51
[16] Hussain, Z., *et al*., A Mathematical Model for Radiative Peristaltic Flow of Jeffrey Fluid in Curved Channel with Joule Heating and Different Walls: Shooting Technique Analysis, *Ain Shams Eng. J*., *13* (2022), 5, 101685
[17] Ullah, H., *et al*., Numerical Treatment of Squeezed MHD Jeffrey Fluid-flow with Cattaneo Chrisstov Heat Flux in a Rotating Frame using Levnberg-Marquard Method, *Alex. Eng. J*., *66* (2023), Mar., pp. 1031-1050
[18] Ibrahim, M. G., Abou-Zeid, M. Y.,Computational Simulation for MHD Peristaltic Transport of Jeffrey Fluid with Density-Dependent Parameters, *Sci. Rep*., *13* (2023), 1, 9191
[19] Naganthran, K., *et al*., Effects of Heat Generation/Absorption in the Jeffrey Fluid Past a Permeable Stretching/Shrinking Disc, *Journal Braz. Soc. Mech. Sci. Eng*., *41* (2019), Sept., 414
[20] Murali, G., Babu, N. V. N., Convective MHD Jeffrey Fluid-flow Due to Vertical Plates with Pulsed Fluid Suction: Numerical Study, *Journal Comput. Appl. Mech*., 54 (2023), 1, pp. 36-48
[21] Narasimhan, T. N., Fourier's Heat Conduction Equation: History, Influence, and Connections, *Rev. Geophys*., *37* (1999), 1, pp 151-172
[22] Christov, C. I., On Frame Indifferent Formulation of the Maxwell-Cattaneo Model of Finite-Speed Heat Conduction, *Mech. Res. Commun.*, *36* (2009), 4, pp. 481-486
[23] Han, S., *et al*., Coupled Flow and Heat Transfer in Viscoelastic Fluid with Cattaneo-Christov Heat Flux Model, *Appl. Math. Lett*., *38* (2014), Dec., pp. 87-93
[24] Hayat, T., *et al.*, Impact of Cattaneo-Christov Heat Flux in Jeffrey Fluid-Flow with Homogeneous-Heterogeneous Reactions, *PLoS ONE*., *11* (2016), 2, 0148662
[25] Siri, Z., *et al*., Heat Transfer over a Steady Stretching Surface in the Presence of Suction, *Bound. Value Probl*., *126* (2018), Aug., 126
[26] Ibrahim, W., *et al.*, Analysis of Flow of Visco-Elastic Nanofluid with Third Order Slips Flow Condition, Cattaneo-Christov Heat and Mass Diffusion Model, *Propuls. Power Res.*, *10* (2021), 2, pp. 180-193
[27] Islam, S., *et al*., Cattaneo-Christov Theory for a Time-Dependent Magnetohydrodynamic Maxwell Fluid-flow through a Stretching Cylinder, *Adv. Mech. Eng*., *13* (2021), 7, pp. 1-11
[28] Tassaddiq, A., Impact of Cattaneo-Christov Heat Flux Model on MHD Hybrid NanoMicropolar Fluid-flow and Heat Transfer with Viscous and Joule Dissipation Effects, *Sci. Rep*., *11* (2021), 1, 67
[29] Makinde, O. D., *et al*., Numerical Exploration of Cattaneo-Christov Heat Flux and Mass Transfer in Magnetohydrodynamic Flow over Various Geometries, *Defect Diffus Forum*., *374* (2017), Apr., pp. 67-82
[30] Ramandevi, B., *et al*., Combined Influence of Viscous Dissipation and Non-Uniform Heat Source/Sink on MHD Non-Newtonian Fluid-Flow with Cattaneo-Christov Heat Flux, *Alex. Eng. J*., *57* (2018), 2, pp. 1009-1018
[31] Arpaci, V. S., *et al*., *Convection Heat Transfer*, Prentice Hall, New Jersey, USA, 1984
[32] Ijaz, M., Ayub, M., Thermally Stratified Flow of Jeffrey Fluid with Homogeneous-Heterogeneous Reactions and Non-Fourier Heat Flux Model, *Heliyon*, *5* (2019), 8, e02303
[33] Tibullo, V., Zampoli, V., A Uniqueness Result for the Cattaneo-Christov Heat Conduction Model Applied to Incompressible Fluids, *Mech. Res. Commun*., *38* (2011), 1, pp. 77-79
[34] Khan, U., *et al.*, On the Cattaneo-Christov Heat Flux Model and OHAM Analysis for Three Different Types of Nanofluids, *Appl. Sci*., *10* (2020), 3, pp. 886-900
[35] White, R. E., Subramanian, V. R., Boundary Value Problems: in *Computational Methods in Chemical Engineering with Maple*, Springer, Berlin, Heidelberg, Germany, 2010

[36] Andersson, H. I., *et al*., Magnetohydrodynamic Flow of a Power-Law Fluid over a Stretching Sheet, *Int. J. Non-Linear Mech*., *27* (1992), 6, pp. 929-936
[37] Chen, C. H., Effects of Magnetic Field and Suction/Injection on Convection Heat Transfer of Non-Newtonian Power-Law Fluids Past a Power-Law Stretched Sheet with Surface Heat Flux, *Int. J. Thermal Science*., *47* (2008), 7, pp. 954-961
[38] Babu, D. H., Narayana, P. S., Joule Heating Effects on MHD Mixed Convection of a Jeffrey Fluid over a Stretching Sheet with Power Law Heat Flux: A Numerical Study, *Journal Magn. Magn. Mater.*, *412* (2016), Aug., pp. 185-193
[39] Hayat, T., *et al.*, Unsteady Flow and Heat Transfer of Jeffrey Fluid over a Stretching Sheet, *Thermal Science*, *18* (2014), 4, pp. 1069-1078

Paper submitted: October 13, 2022
Paper revised: May 14, 2023
Paper accepted: October 13, 2023